Rate Coefficients and Final States for the Dissociative Recombination of LiH^+

S. Krohn,[1,2] M. Lange,[2] M. Grieser,[2] L. Knoll,[2,1] H. Kreckel,[2] J. Levin,[2] R. Repnow,[2] D. Schwalm,[2] R. Wester,[2] P. Witte,[1,2] A. Wolf,[2] and D. Zajfman[1]

[1]*Department of Particle Physics, Weizmann Institute of Science, Rehovot, 76100, Israel*

[2]*Max-Planck-Institut für Kernphysik, D-69029 Heidelberg, Germany*

(Received 19 December 2000)

The dissociative recombination of LiH^+ ions with low-energy electrons is observed at a storage ring and the final states are analyzed using fragment imaging and field ionization techniques. The rate coefficient is found to be larger than its estimated value used in astrophysical models. Mostly the highest energetically possible Rydberg states of the lithium atom are populated by the reaction, indicating a common trend for molecular recombination via the noncrossing mode.

DOI: 10.1103/PhysRevLett.86.4005 PACS numbers: 34.80.Lx, 52.20.Hv, 95.30.Dr, 98.80.Bp

Among the molecules which were created in the early universe during the recombination era, LiH is of particular interest because of its contribution to the cooling of the primordial gas and its possible effects on the cosmic blackbody background radiation. However, as a result of its low ionization potential, lithium remained almost fully ionized at the time of hydrogen recombination. Thus, lithium chemistry in the early universe might have been initiated by the radiative association process forming LiH^+ molecules [1,2]. On the other hand, the resulting LiH^+ abundance is assumed to be limited by photoionization, collisions, and dissociative recombination (DR) with free electrons [3–5]. This latter process can, for low-energy electrons, be depicted as

$$LiH^+(v) + e^-(E) \rightarrow Li(nl) + H(1s) + E_k\,, \qquad (1)$$

where v, n, and l denote the initial vibrational state of the molecular ion and the principal and orbital quantum numbers of the Li product, respectively, while E_k is the kinetic energy release. From existing calculations of the LiH and LiH^+ molecular potential curves [6,7], it does not appear that any doubly excited neutral state would cross the ionic ground-state potential, in contrast to most other diatomic molecular ions [8,9] where generally such a crossing leads to high DR rates. The absolute DR rate coefficient for LiH^+ to our knowledge has never been measured, and only an estimated value of 2.6×10^{-8} cm^3 s^{-1} at 300 K, rather low as compared to many other molecular ions, has been used in early universe models [3].

LiH^+ presumably, together with HeH^+, figures among the very few diatomic ions that recombine with slow electrons via noncrossing processes [10,11]. Beside its important role in astrophysics, the DR of LiH^+ therefore is of considerable interest also in the context of basic molecular processes. Other uncommon characteristics of LiH^+ are the low dissociation energy (~116 meV from the $v = 0$ level in the $X^2\Sigma^+$ ground-state potential) and the small ionization energy of 5.39 eV of atomic lithium. These circumstances lead to an exceptionally large number of energetically allowed final states for the neutral Li fragment, where (see Fig. 1) Rydberg levels up to $11s$ can be reached even from the $v = 0$ level at near-zero electron energy. Moreover, the vibrational energy spacings of LiH^+ are so small that already at moderate temperature several excited vibrational levels are thermally populated and yet higher Rydberg levels can be reached energetically by recombination with slow electrons.

In this Letter, we present the first experimental result for the absolute DR rate coefficient of LiH^+, as well as a measurement of final-state populations by fragment imaging and by state-selective field ionization. A stored LiH^+ ion beam is used whose internal excitation can be assumed to be in equilibrium with the environment at ~300 K, yielding almost 80% of the ions in the vibrational ground state.

The experiment was carried out at the heavy-ion storage ring TSR located at the Max-Planck-Institut für Kernphysik, Heidelberg, Germany. The $^7LiH^+$ ion beam was produced in a Tandem accelerator by gas stripping and dissociation of LiH_2^- ions from a cesium sputter source.

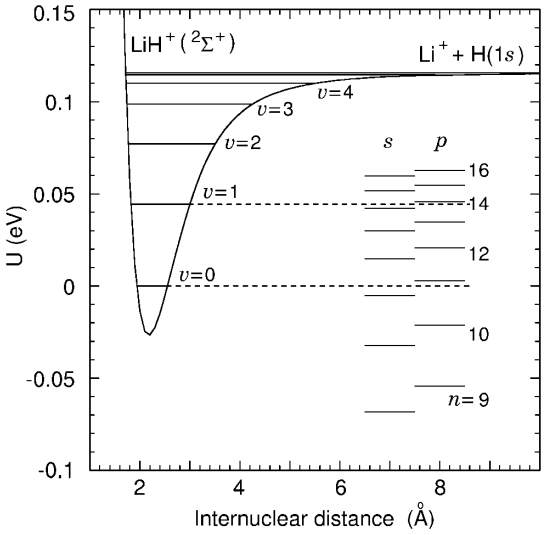

FIG. 1. Potential energy curve for the $X^2\Sigma^+$ state of the LiH^+ molecule (Berriche *et al.* [7]) with positions of the vibrational levels and the fragment energy levels for the H(1s) + Li(nl) channel with $l = 0$ and 1 (s and p).

After acceleration to an energy of 6 MeV and magnetic mass selection, the beam was injected into the TSR and kept circulating for up to about 17 s. In a straight section of the ring, the ion beam (initial diam. $\sim$2 cm) was merged with a collinear electron beam of $\sim$1.5 cm diam. over an interaction region of 1.5 m length (2.7% of the ring circumference). The electron beam was guided by a longitudinal magnetic field of 0.04 T, and toroidal inflectors where the guiding field was bent with a radius of 0.8 m were used to merge and demerge electron and ion beams. The motional electric field due to stray transverse components of the magnetic guiding field in the straight overlap region amounted to $\lesssim$3 V/cm. The stored LiH^+ ion beam was electron cooled during $\sim$5 s after the injection by Coulomb collisions in the two overlapping beams at matched velocities, yielding an ion beam diameter of $\lesssim$2 mm and a relative momentum spread of $\lesssim 10^{-4}$. The electron beam was then used as an electron target for the DR experiment. At matched average beam velocities, it supplied free electrons with a density of 8.5×10^6 cm^{-3} and with kinetic energies relative to the LiH^+ ions as characterized by the longitudinal and transversal electron temperatures of $kT_\parallel = 0.1$ meV and $kT_\perp = 12$ meV, respectively. The LiH^+ beam lifetime was $\sim$13 s when the electron beam was turned off and $\sim$5 s with the velocity-matched electron beam turned on.

The fragments resulting from the DR of LiH^+ ions, as well as from their collisions with the background gas at $\sim 5 \times 10^{-11}$ mbar, were detected behind the first bending dipole magnet following the interaction region (see Fig. 2), about 6.5 m downstream from the center of the electron beam section. The neutral fragments passed straight through the dipole and were analyzed either by a spatially nonresolving surface barrier detector (SBD) or by a microchannel plate (MCP) providing event-by-event imaging of the fragments. By its energy resolution, the SBD could distinguish events where pairs of neutral Li and H atoms were produced from events yielding only single Li or H atoms. Li fragments reaching the dipole magnet (field strength $\sim$0.87 T) in Rydberg states $n \geq 8$ are expected to be field ionized by its strong ($\sim$100 kV/cm) motional electric field. The Li^+ ions produced by interactions with the background gas or by field ionization of neutral Li fragments were counted on a spatially resolving, movable MCP detector located on the inner side of the closed ion orbit (see Fig. 2). All measurements described below were obtained after storing and electron cooling the LiH^+ ions for $>$7 s. The vibrational lifetimes derived from calculated transition dipole moments [12] indicate that this time should be sufficient to reach thermal equilibrium with the storage ring walls ($T \sim 300$ K) with relative populations of $\sim$78% in $v = 0$, $\sim$14% in $v = 1$, and $\sim$8% in higher levels.

By changing the electron beam acceleration voltage while keeping the ion energy constant, the relative energy of electrons and ions was varied from zero up to several eV. Tuning to zero relative energy yielded a large rate

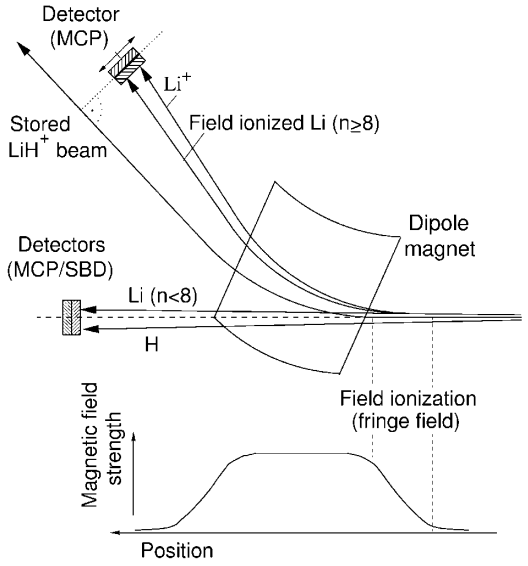

FIG. 2. Schematic of the detector arrangement and the principle of analyzing the field ionization of Li fragments. The ionization point in the linearly rising fringe field of the dipole is reflected by the impact position of the field ionization product on the MCP detector.

of single H fragments, as observed on the SBD, which dropped to $\sim 1/4$ of the maximum value already at 5 meV and to $<$3% at 50 meV. A signal with the same energy dependence, but with a maximum of only $\sim$15% of the H signal, was observed for Li and H fragment pairs (full beam energy in the SBD). We assign both the H and the Li + H signal as being due to low-energy DR and explain the occurrence of a single H fragment in $\sim$85% of all events by field ionization of Rydberg ($n \geq 8$) Li atoms in the dipole magnet (see below). In separate measurements the decrease of the LiH^+ beam current was monitored, using the time dependence of the H fragment yield (as a signal proportional to the ion beam current) to derive the loss rate of LiH^+ ions. The increase of this loss rate on tuning the relative electron-ion energy from values $\gtrsim$100 meV to zero was measured to be (0.14 ± 0.05) s^{-1}. From the electron density and the ratio of the electron-ion interaction region to the ring circumference we derive a DR rate coefficient of $\alpha_{\mathrm{mb}} = (6 \pm 2) \times 10^{-7}$ cm^3 s^{-1}, pertaining to our merged-beam conditions with the anisotropic thermal distribution at $kT_\perp = 12$ meV and $kT_\parallel = 0.1$ meV (see above). On the assumption that the DR cross section varies as $\propto 1/E$, this can be converted to a thermal rate coefficient (isotropic Maxwell-Boltzmann distribution) of $\alpha = (3.8 \pm 1.4) \times 10^{-7}$ cm^3 s^{-1} at 300 K.

Two methods were applied to analyze the Li fragment states formed in the DR process at zero relative beam energy. First, similar to DR experiments on other diatomic molecular ions [13], the distance between pairs of neutral products was measured using event-by-event fragment imaging on the zero-degree MCP detector (see Fig. 2). For an ensemble of events leading to the same final channel,

the associated kinetic energy release is reflected by the spatial extent of the transverse-distance distribution, while the shape of this distribution results from an average over the interaction region and the dissociation angles [13]. The neutral Li and H fragment pairs which are not affected by field ionization and thus can reach the imaging detector show a projected distance distribution (see Fig. 3) which reveals that Li fragments in states with $n \leq 5$ are essentially absent ($\lesssim$1% of the total counts in the fragment distance spectrum) and that final channels up to $n \sim 10$ are more and more populated as n increases. The observation that a significant fraction ($\sim$15% according to the SBD measurements described above) of the Li atoms formed in high ($n \geq 8$) Rydberg states can escape field ionization is consistent with the calculated radiative lifetimes of Li Rydberg states [14], which for $n = 8-10$ and $l = 0$ are comparable with the time of flight from the electron cooler to the dipole magnet of $\sim$500 ns.

Second, the spatially resolved observation of the Li^+ fragments behind the dipole magnet allowed us to distinguish the ions generated by field ionization of Li recombination products from those directly produced by the dissociation of LiH^+ in background gas collisions. While the directly produced Li^+ ions are bent immediately on entering the fringe field of the dipole magnet, the Li atoms that undergo field ionization first continue on a straight trajectory over a distance of several cm until they reach a point where the motional electric field becomes high enough to cause field ionization (see Fig. 2). Hence, through the missing deflection in the fringe field before ionization, the impact position of field-ionized DR fragments at the MCP detector becomes dependent on the ionization field strength. The DR fragments are, in fact, distributed over a band of $\sim$10 cm, which was imaged by the position-resolving MCP (2.5 cm active diam.) in several measurements with overlapping observation ranges (applying cross normalization through the H count rate on the zero-degree SBD).

Position distributions for field-ionized DR fragments along a scan line parallel to the magnetic bending plane are shown in Fig. 4. The data were transformed from the position scale to a scale representing the ionization field strength of the Li fragment, using numerical trajectory calculations including the fringe field of the TSR dipoles as measured separately; a nearly linear relation exists between the position and the ionization field strength. The zero of the electric field scale was adjusted by shifting the low-field shoulder of the observed distribution to $\sim$7 kV/cm, corresponding to the size of motional electric fields seen by the ions before reaching the dipole. An uncertainty of $\pm$1.5 kV/cm is estimated for the field strength scale. For most of the events in the spectrum of Fig. 4, the field ionization points lie in the near-linear region of the fringe field (cf. Fig. 2), where the field strength rises with a slew rate of $S \sim 4.4$ kV $(\mathrm{cm\,ns})^{-1}$. The critical ionization fields F_c are expected [15] to depend on the initial quantum state of the Li atom as well as on the quantum mechanical time evolution of the system during the field ramp, proceeding through numerous avoided level crossings. The magnetic field of the bending dipole also experienced by the Li atoms gives rise to comparatively small perturbations with typical interaction energies estimated to be $\lesssim$0.1 of the level splittings induced by the motional electric field for levels with $n \sim 10$.

Conclusions about the Rydberg state populations can be obtained from the field ionization spectrum on the basis of the semiclassical scaling law $F_c = C/n^4$ [15]. Neglecting all energy shifts by the electric field and equating the field-free binding energy of a Rydberg level n to the location of the saddle point in the combined Coulomb and external potentials, a value of $1/16$ is obtained for the scaling parameter C. Considering the quantum mechanical evolution of a low-l initial Rydberg state, as calculated for Li ($n = 19$) by Rubbmark *et al.* [16], along a completely adiabatic path to the field ionization limit, ionization should take place at only slightly higher fields, as described by $C \sim 1/12.8$. On the other hand, the completely diabatic evolution of a low-l initial state through the field region where avoided crossings between different n manifolds occur [16] would lead to much higher ionization fields with $C \sim 1/9$ [15]. We find that the scaled critical fields

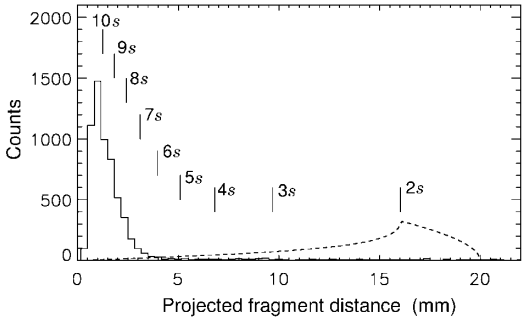

FIG. 3. Histogram of observed projected distances of neutral Li and H fragments, measured between 7 to 11 s after injection, and the expected shape of the histogram for the Li($2s$) final channel (dashed line). Also indicated are the maxima of the expected distributions from higher final states.

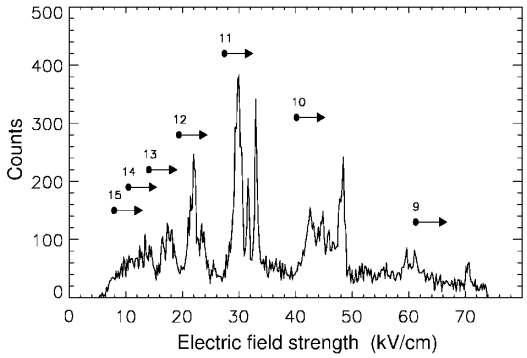

FIG. 4. Field ionization spectrum taken between 7 and 11 s after injection. Critical field strengths $F_c = C/n^4$ with $C = 1/12.8$ (see text) are indicated for various n.

F_c with $C = 1/12.8$, marked in Fig. 4, yield spacings in reasonable agreement with the low-field limits of several multiplets in our field ionization spectrum, which we thus assign to initial Li Rydberg states n as indicated. The peak structure in the n multiplets is likely to originate from systems that reach the n-manifold crossing region in different sublevels and evolve adiabatically to the field ionization limit; at this stage of the work we have not performed the elaborate case-specific calculations that would be needed to understand this peak structure in detail. The diffuse tails of the multiplets towards higher ionization fields probably correspond to systems evolving via random alternative paths where the level crossings are partly traversed diabatically. Indeed, using the critical slew rate (where distribution of flow by diabatic transitions starts in the n manifold crossing region) of ~ 0.02 kV(cm ns)$^{-1}$ by Rubbmark *et al.* [16] for Li ($n = 19$) and the scaling $\propto n^{-10}$ that results from Eq. (7.6) of Ref. [15], we expect diabatic transitions to set in at our slew rate for $n \gtrsim 11$.

Based on this interpretation of the field ionization spectrum, the DR of LiH^+ ions with low-energy electrons appears to populate predominantly Rydberg levels of neutral Li with $n \sim 10-12$. The field ionization analysis, of course, is not sensitive to the population of lower levels ($n \leq 8$); however, the fragment imaging results discussed above indicate that such levels indeed are not populated significantly. Hence, our results clearly demonstrate the strong tendency for this system to produce, among all the energetically accessible states, the *highest possible* excited fragments (cf. Fig. 1).

Lacking a doubly excited neutral dissociating potential crossing the ground electronic state of the ion, the DR reaction has to take place by a direct coupling to the Rydberg states located below the ionic core. Based on the ideas developed by Guberman [10] and Sarpal, Tennyson, and Morgan [11] for the noncrossing DR mode, such single-electron radiationless transitions can be mediated by nonadiabatic coupling if Rydberg states change their character at internuclear distances in the range of the ionic vibrational wave function. Such a situation could be shown to exist [10] for HeH^+ and to explain the predominant branching to the final channel $He(1s^2) + H(2l)$, as observed by DR experiments [17,18]. Experiments on HeH^+ also showed [18] that the final-state population after DR switched almost completely to $H(3l)$ as soon as electron energies were reached for which this exit channel was open. The present findings for LiH^+ seem to continue this trend to the extreme case of very high Rydberg levels which are already open at low electron energy for this system. Calculated potential curves of LiH Rydberg levels (so far for up to $n = 4$ [6]) indeed indicate strong nonadiabatic coupling between the Rydberg states at internuclear distances in the region of the LiH^+ vibrational states. Our results suggest that efficient nonadiabatic coupling continues to exist in the relevant internuclear distance region up to very high molecular Rydberg levels, which leads to sizable rates for recombination processes that populate the highest energetically accessible final states.

Apart from the results on the final states, also a first experimental value of the rate coefficient for the DR of LiH^+ with low-energy electrons has been obtained in this study. The present result is more than 1 order of magnitude larger than the rate assumed in early universe models [3]. However, it is important to recall that the applied LiH^+ ion beam, although in thermal equilibrium with the 300 K experimental surrounding, is still expected to be in a superposition of vibrational states as specified above. On the other hand, the present rate coefficient promotes the DR process to be the fastest reaction among all those taken into account in the different models (see Table I in Ref. [3]). We hope that further theoretical calculations will provide more insight into both the unusual final state populations and the unexpected large rate coefficient measured here.

Support of this project by the German Federal Ministry of Education and Research (BMBF) within the framework of the German-Israeli Project Cooperation (DIP) is gratefully acknowledged.

[1] A. Dalgarno, K. Kirby, and P. C. Stancil, Astrophys. J. **458**, 397 (1996).
[2] F. A. Gianturco and G. Giorgi, Astrophys. J. **479**, 560 (1997).
[3] P. C. Stancil, S. Lepp, and A. Dalgarno, Astrophys. J. **458**, 401 (1996).
[4] D. Galli and F. Palla, Astron. Astrophys. **335**, 403 (1998).
[5] K. Kirby, Phys. Scr. **T59**, 59 (1995).
[6] A. Boutalib and F. X. Gadéa, J. Chem. Phys. **97**, 1144 (1992).
[7] H. Berriche and F. X. Gadéa, Chem. Phys. **191**, 119 (1995).
[8] D. R. Bates and H. S. W. Massey, Proc. R. Soc. London **192**, 1 (1947).
[9] J. N. Bardsley, J. Phys. B **1**, 349 (1968); **1**, 365 (1968).
[10] S. Guberman, Phys. Rev. A **49**, R4277 (1994).
[11] B. K. Sarpal, J. Tennyson, and L. A. Morgan, J. Phys. B **27**, 5943 (1994).
[12] F. A. Gianturco, P. G. Giorgi, H. Berriche, and F. X. Gadea, Astron. Astrophys. Suppl. Ser. **117**, 377 (1996).
[13] Z. Amitay *et al.,* Phys. Rev. A **54**, 4032 (1996).
[14] C. Theodosiou, Phys. Rev. A **30**, 2881 (1984).
[15] T. Gallagher, *Rydberg Atoms* (Cambridge University Press, Cambridge, 1994).
[16] J. R. Rubbmark, M. M. Kash, M. G. Littman, and D. Kleppner, Phys. Rev. A **23**, 3107 (1981).
[17] T. Tanabe *et al.,* Phys. Rev. A **49**, R1531 (1994).
[18] J. Semaniak *et al.,* Phys. Rev. A **54**, R4617 (1996).